Supporting Information

A family of quasi-one-dimensional zigzag spin chain compounds $Ba_2REV_3O_{11}$ (RE = Pr, Nd, and Gd-Ho)

Jin Zhou,[a] Tong Shi,[a] Ri-Tao Huang,[a] An-Di Liu,[a] Gao-Shang Gong,[b] Yong-Qiang Wang,[b] Lang-Sheng Ling,[c] Jing-Xin Li,[c] Yu-Yan Han,[c] Wei Tong,[c] Zheng-Cai Xia,[a] Zhao-Ming Tian,*[a]

[a] School of Physics and Wuhan National High Magnetic Field Center, Huazhong University of Science and Technology, Wuhan, Hubei, 430074, China
[b] Zhengzhou University of Light Industry, School of Electronics & Information, Zhengzhou, Henan, 450002, China
[c] Anhui Key Laboratory of Low-energy Quantum Materials and Devices, High Magnetic Field Laboratory, HFIPS, Chinese Academy of Sciences, Hefei, Anhui, 230031, China

1. The crystal structure information of $Ba_2REV_3O_{11}$ (RE = Pr, Nd, Gd-Ho)

Room temperature experimental and refined powder X-ray diffraction (XRD) spectra for the synthesized $Ba_2REV_3O_{11}$ (RE = Pr, Nd, Gd-Ho) samples are shown in Figure S1, and all the diffraction peaks can be indexed by the monoclinic structure with *P*21/*a* space group without any detected impurity phases. The calculated XRD patterns match well with the experimental data with small values of reliability factors R_p (4.94-3.86) and R_{wp} (5.83-4.56). From the structure refinements, the extracted structural parameters are listed in Table S1 and S2.

2. The low temperature dc and ac magnetic susceptibility of $Ba_2DyV_3O_{11}$

The low temperature magnetic susceptibility χ(T) curves under different fields from 0.05 T to 0.3 T for $Ba_2DyV_3O_{11}$ are shown in Figure S2. As seen, the χ(T) measured at low fields show a magnetic anomaly at ~ 3.0 K. From the differential magnetic susceptibility dχ/dT curves shown in Figure S2(b), the transition peak is determined to be at ~2.9 K. To further confirm the existence of magnetic transition, the real part of *ac* susceptibility curves of $Ba_2DyV_3O_{11}$ at various frequencies are presented in Figure S3(a). The broad peak maximized at T_p~3.0 K is observed, which shows weak frequency dependence indicative of long range magnetic order. Also, the specific heat reveals a clear λ-like anomaly at ~2.9 K. Below~2.9 K, the heat capacity continues to rise possibly due to the presence of an additional magnetic transition at lower temperatures, similar to observations in other RE-based magnets reported in $Ho_3Al_5O_{12}$ and $DyBO_3$ compounds[1,2].

References

1. S. Nagata, H. Sasaki, K. Suzuki, J. Kiuchi, N. Wada, Specific heat anomaly of the holmium garnet $Ho_3Al_5O_{12}$ at low temperature, *J. Phys. Chem. Solids*, 2001, **62**, 1123-1130.
2. P. Mukherjee, Y. Wu, G.I. Lampronti, S.E. Dutton, Magnetic properties of monoclinic lanthanide orthoborates, $LnBO_3$, Ln = Gd, Tb, Dy, Ho, Er, Yb, *Mater. Res. Bull*, 2018, **98**, 173-179.

Table S1. The selected bond distances, bond angles of $Ba_2REV_3O_{11}$(RE = Pr, Nd, Gd-Ho) polycrystals

RE	Pr	Nd	Gd	Tb	Dy	Ho
Crystal system	Monoclinic	Monoclinic	Monoclinic	Monoclinic	Monoclinic	Monoclinic
Space group	P21/c	P21/c	P21/c	P21/c	P21/c	P21/c
Intra-chain RE-RE (Å)	3.952(3)	3.947(4)	3.875(2)	3.866(3)	3.859(2)	3.856(2)
Inter-chain RE-RE (Å)	5.245(3)	5.235(2)	5.216(2)	5.202(4)	5.195(3)	5.191(4)
	5.974(2)	5.965(4)	5.954(1)	5.923(3)	5.917(3)	5.913(4)
RE-O1 (Å)	2.691(2)	2.684(2)	2.667(3)	2.656(2)	2.651(1)	2.648(2)
RE-O1 (Å)	2.303(1)	2.276(1)	2.243(2)	2.195(2)	2.192(1)	2.187(1)
RE-O2 (Å)	2.537(2)	2.372(1)	2.342(3)	2.286(2)	2.244(1)	2.218(2)
RE-O2 (Å)	3.112(2)	2.965(4)	2.642(4)	2.594(2)	2.588(2)	2.583(1)
RE-O4 (Å)	3.084(2)	3.063(1)	3.043(4)	3.032(3)	3.030(2)	3.022(2)
RE-O11 (Å)	2.221(2)	2.346(1)	2.853(4)	3.012(4)	3.014(2)	3.135(2)
RE-O1-RE (°)	105.763(5)	105.426(6)	105.383(4)	105.264(6)	105.215(5)	105.197(4)
RE-O2-RE (°)	107.877(6)	107.815(4)	107.764(7)	107.657(6)	107.553(5)	107.516(4)
V1-O1 (Å)	1.821(3)	1.814(3)	1.786(4)	1.774(2)	1.771(2)	1.768(1)
V1-O2 (Å)	1.795(2)	1.785(4)	1.780(5)	1.772(4)	1.770(2)	1.774(2)
V1-O3 (Å)	1.773(4)	1.725(3)	1.572(4)	1.561(5)	1.559(6)	1.558(6)
V1-O5 (Å)	1.871(2)	1.837(3)	1.806(3)	1.729(1)	1.725(6)	1.724(4)
V2-O6 (Å)	1.832(1)	1.803(2)	1.798(4)	1.782(2)	1.781(4)	1.779(3)
V2-O8 (Å)	1.756(2)	1.745(2)	1.683(3)	1.634(2)	1.632(4)	1.631(4)
V2-O10 (Å)	1.772(3)	1.755(3)	1.738(3)	1.708(2)	1.704(3)	1.704(3)
V2-O11 (Å)	1.784(2)	1.764(2)	1.732(4)	1.706(4)	1.703(3)	1.702(3)
V3-O4 (Å)	1.728(2)	1.721(2)	1.715(3)	1.714(4)	1.712(2)	1.710(4)
V3-O6 (Å)	1.805(2)	1.833(2)	1.793(3)	1.788(2)	1.784(3)	1.782(4)
V3-O7 (Å)	1.632(1)	1.649(3)	1.751(3)	1.618(3)	1.617(3)	1.616(4)
V3-O9 (Å)	1.685(3)	1.701(3)	1.696(4)	1.667(2)	1.663(3)	1.661(3)
V2-O6-V3 (°)	167.424(3)	167.455(1)	167.494(2)	167.412(4)	167.415(3)	167.402(3)
Ba1-O3(Å)	3.212(2)	3.197(1)	3.194(4)	3.190(3)	3.185(4)	3.181(2)
Ba1-O4(Å)	3.343(2)	3.337(4)	3.312(4)	3.277(3)	3.266(2)	3.264(2)
Ba1-O5 (Å)	2.724(4)	2.710(1)	2.704(4)	2.695(4)	2.692(3)	2.690(2)
Ba1-O7 (Å)	2.989(2)	2.976(1)	2.951(3)	2.947(3)	2.942(3)	2.942(4)
Ba1-O8 (Å)	3.423(2)	3.413(4)	3.399(3)	3.397(4)	3.393(2)	3.391(3)
Ba1-O9 (Å)	2.842(2)	2.836(3)	2.807(3)	2.799(2)	2.793(2)	2.791(2)
Ba1-O10 (Å)	2.911(3)	2.895(2)	2.852(4)	2.846(3)	2.838(2)	2.833(2)

Ba1-O11 (Å)	2.938(2)	2.921(3)	2.849(4)	2.794(2)	2.791(2)	2.779(2)
Ba2-O5(Å)	2.879(2)	2.796(2)	2.752(3)	2.788(2)	2.784(3)	2.781(3)
Ba2-O7(Å)	2.877(3)	2.848(2)	2.818(4)	2.756(2)	2.749(2)	2.746(2)
Ba2-O7 (Å)	3.313(2)	3.325(2)	3.471(4)	3.454(3)	3.452(2)	3.454(2)
Ba2-O8 (Å)	2.806(3)	2.893(3)	3.017(3)	2.964(2)	2.972(4)	2.976(4)
Ba2-O8 (Å)	3.035(3)	3.004(1)	3.032(4)	2.874(2)	2.867(3)	2.868(4)
Ba2-O9 (Å)	3.004(2)	2.947(2)	3.063(4)	3.103(3)	3.096(2)	3.102(2)
Ba2-O9 (Å)	2.897(2)	2.956(3)	2.976(3)	3.078(4)	3.073(2)	3.069(2)
Ba2-O10 (Å)	3.126(2)	3.093(1)	2.974(3)	2.781(2)	2.776(1)	2.775(1)
Ba2-O10 (Å)	3.113(3)	2.961(2)	2.894(1)	2.833(2)	2.827(1)	2.824(1)

Table S2. The crystallographic parameters of $Ba_2REV_3O_{11}$ (RE = Pr, Nd, Gd-Ho) from the structural refinements on room temperature powder XRD spectra.

	Pr	**Nd**	**Gd**	**Tb**	**Dy**	**Ho**
Crystal system	Monoclinic	Monoclinic	Monoclinic	Monoclinic	Monoclinic	Monoclinic
Space group	P21/a	P21/a	P21/a	P21/a	P21/a	P21/a
a(Å)	12.418(5)	12.399(7)	12.342(5)	12.319(6)	12.314(5)	12.305(6)
b(Å)	7.767(5)	7.754(4)	7.707(6)	7.688(5)	7.683(6)	7.672(5)
c(Å)	11.246(7)	11.218(8)	11.152(6)	11.125(9)	11.116(8)	11.105(7)
Volume($Å^3$)	1056.794(19)	1050.656(16)	1033.103(18)	1025.617(21)	1023.186(22)	1019.743(20)
α=γ(degree)	90	90	90	90	90	90
β(degree)	103.021(3)	103.052(4)	103.116(2)	103.242(6)	103.365(4)	103.417(3)
χ^2	1.087	1.042	1.694	1.077	1.515	1.264
R_{wp}	5.54	5.83	5.66	5.42	4.56	5.15
R_p	4.94	4.75	4.14	4.29	3.86	4.35

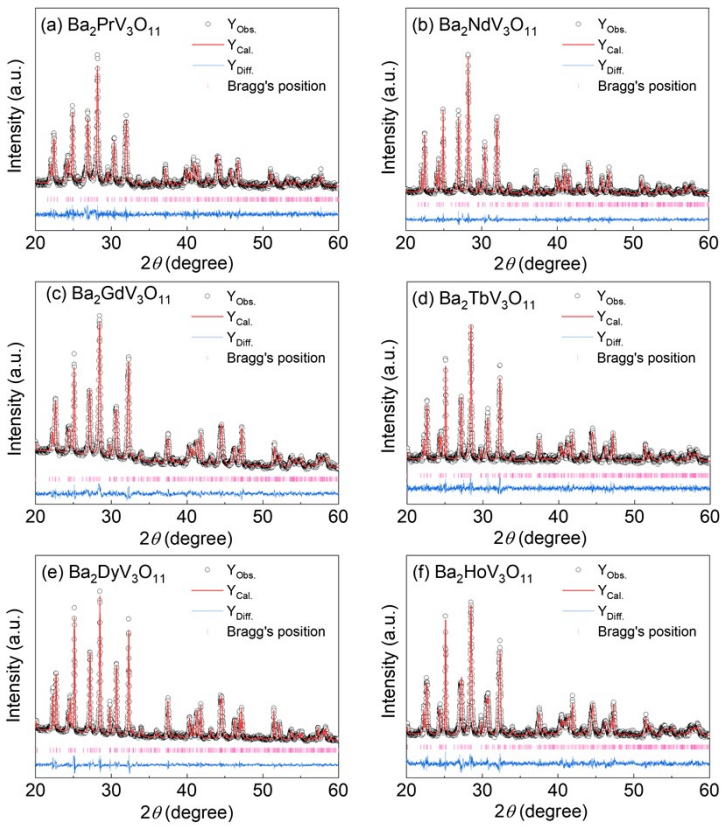

Figure S1. Room-temperature powder X-ray diffraction (XRD) spectra of $Ba_2REV_3O_{12}$ (RE = Pr, Nd, Gd-Ho) samples: the black cycles denote the experimental data, red and blue lines are the calculated patterns and its difference with the experimental data, the pink stick reflect the Bragg reflection positions.

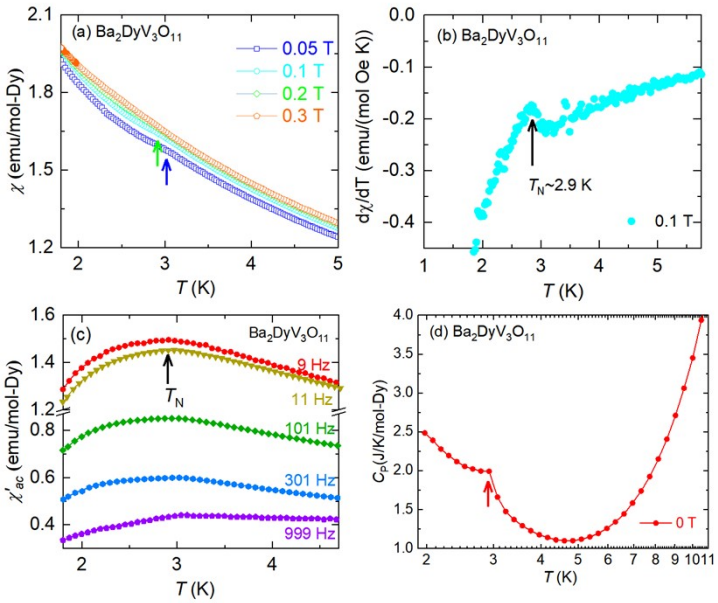

Figure S2. (a) Temperature dependence of magnetic susceptibility χ(T) under different

magnetic fields for $Ba_2DyV_3O_{11}$. (b) The differential magnetic susceptibility dχ/dT curves under field of 0.1 T. (c) The real part of *ac* susceptibility (χ'_{ac}) at various frequencies of $Ba_2DyV_3O_{11}$. (d) The zero-field specific heat C_p(T) curves of $Ba_2DyV_3O_{11}$